

FedProtoKD: Dual Knowledge Distillation with Adaptive Class-wise Prototype Margin for Heterogeneous Federated Learning

Md Anwar Hossen*, Fatema Siddika*, Wensheng Zhang, Anuj Sharma, Ali Jannesari
Department of Computer Science, Iowa State University, Ames, USA
{manwar, fatemask, wzhang, anuj_s, jannesar}@iastate.edu

Abstract—Heterogeneous Federated Learning (HFL) has gained attention for its ability to accommodate diverse models and heterogeneous data across clients. Prototype-based HFL methods emerge as a promising solution to address statistical heterogeneity and privacy challenges, paving the way for new advancements in HFL research. This method focuses on sharing only class-representative prototypes among heterogeneous clients. However, these prototypes are often aggregated on the server using weighted averaging, leading to sub-optimal global knowledge; these cause the shrinking of aggregated prototypes, which negatively affects the model performance in scenarios when models are heterogeneous and data distributions are extremely non-IID. We propose FedProtoKD in a Heterogeneous Federated Learning setting, using an enhanced dual-knowledge distillation mechanism to improve the system performance with clients’ logits and prototype feature representation. We aim to resolve the prototype margin-shrinking problem using a contrastive learning-based trainable server prototype by leveraging a class-wise adaptive prototype margin. Furthermore, we assess the importance of public samples using the closeness of the sample’s prototype to its class representative prototypes, which enhances learning performance. FedProtoKD achieved average improvements of 1.13% up to 34.13% accuracy across various settings and significantly outperforms existing state-of-the-art HFL methods.

Index Terms—Heterogeneous model, Margin Shrinking, Contrastive Learning, Adaptive Prototype Margin, and Knowledge Distillation.

I. INTRODUCTION

Federated learning (FL) represents a significant breakthrough in machine learning, enabling decentralized model training while protecting data privacy. However, traditional FL methods such as FedAvg [1] suffer from performance degradation due to statistical heterogeneity [2], [3]. To address this issue, personalized FL [2] approaches were developed to learn personalized model parameters for each client. However, most of these methods assume that all clients use the same model architecture and communicate their model updates to the server for training a shared global model [4]–[6]. This approach not only leads to high communication costs [7] but also exposes client models, raising concerns about privacy and intellectual property (IP) [8]–[10].

To address these challenges, heterogeneous FL (HFL) [11] has emerged as an innovative FL paradigm that allows clients to use diverse model architectures and handle heterogeneous data without sharing private model parameters. Instead, clients exchange global knowledge, which reduces communication

overhead and enhances model performance. For example, with the federated ensemble distillation method [12] the server utilizes a public set of unlabeled proxy samples to train the global model, aiming to replicate the outputs of the local models on these samples. Since this method does not impose constraints on the model structures used for training or distillation, it effectively handles the heterogeneity introduced by local model drift or differences in model architectures. However, these methods depend highly on the availability and quality of the global dataset [13]. Data-free KD approaches employ auxiliary models as global knowledge [14], [15], but the communication overhead of transmitting these models remains substantial.

Prototype-based HFL methods [11], [16] propose sharing lightweight class representatives, or prototypes, as global knowledge, significantly reducing communication overhead. Amidst the advancement of prototype-based approaches in HFL it faces significant challenges, particularly when aggregating client prototypes on the server through weighted averaging. Heterogeneity among clients leads to prototypes with varying scales and separation margins. When these diverse prototypes are averaged, the global prototypes tend to suffer from a reduction in class margins; this phenomenon is known as the “Prototype Margin Shrink”, which diminishes the distinctiveness and quality of the global prototypes [17]. The prototype margin represents the smallest Euclidean distance between the prototype of a class and the prototypes of other classes. FedPKD [18], a Prototype-Based Ensemble Distillation method, filters knowledge using class-wise prototypes to select proxy samples with high-quality information for distillation. Local clients infer on the unlabeled public dataset and share the logits and prototypes of the local models. In addition, the data sample size for each class is taken to aggregate the prototypes on the server. However, these aggregated prototypes suffer from the prototype’s margin-shrinking problems. Also, filtering out some samples makes the system more biased towards specific samples. In their work, the user has to share the private data sample count (numbers of sample data each client’s local dataset belongs to) to aggregate the representative feature prototype in the server, which is against user privacy. Fed2PKD [19] uses prototypical contrastive distillation to align client embeddings with global prototypes. It also applies semi-supervised global distillation to capture global data characteristics. The method relies on ResNet50, ResNet101,

and ResNet152, all with 2048-dimensional prototype layers (the 2048-dimensional output before the final classification layer). This uniform dimension overlooks models with varying layer sizes. As a result, it limits Fed2PKD’s ability to address federated learning’s heterogeneity challenge.

To overcome the limitations of previous work, our proposed work investigates the benefits of using knowledge distillation with the techniques that mitigate the prototype margin shrinkage problem in HFL. In particular, we designed a novel HFL method called **Federated Prototype-based Dual Knowledge Distillation** (FedProtoKD), which leverages enhanced knowledge distillation. To tackle heterogeneity in federated learning, we employed ResNet18 and ResNet34 with 512-dimensional prototype layers alongside ResNet50, ResNet101, and ResNet152 with 2048-dimensional layers, expanding beyond Fed2PKD’s uniform dimensional approach. We aligned these model dimensions using a learnable projection layer to address model heterogeneity. Furthermore, we designed an **Adaptive Class Wise Margin-Based Trainable Server Prototype** (ACTSP), using a contrastive learning-based generator to generate a trainable server prototype. This trainable server prototype helps the generator to produce class-specific prototypes while maintaining the significant prototype gap, allowing the model to learn the significance of different class prototypes. We prioritized high-quality samples of unlabeled public datasets to improve the accuracy and reliability of the global model. Giving higher importance to samples closer to the aggregated knowledge ensures better alignment with class prototypes, leading to more effective training. Reducing the influence of distant samples prevents noisy or irrelevant data from negatively impacting model performance. Instead of requiring users’ sample counts when aggregating logits, we utilized the variance of logits to preserve individual client privacy.

To evaluate the effectiveness of our FedProtoKD, we conducted extensive experiments in various settings and compared them with state-of-the-art benchmarks. The experimental results show that our proposed FedProtoKD outperforms the learning performance and communication efficiency benchmarks for client and server models under various non-IID settings. Our main contributions can be summarized as follows.

- We propose FedProtoKD, an enhanced prototype-based knowledge distillation framework that addresses model heterogeneity by aligning the models’ varying prototype dimensions through a learnable projection layer and addresses data heterogeneity using a dual knowledge distillation method.
- To solve the prototype margin shrinking problem on the aggregated clients prototype, we generate a trainable server prototype using an adaptive class-wise margin-based approach with the help of contrastive learning. This approach ensures the efficient separability of class prototypes.
- Furthermore, we assess the importance of public samples using the proximity of the sample prototype to the representative class prototypes, which improves servers’

learning performance based on local logits and trainable prototypes.

- We perform comprehensive experiments and extensive comparisons, including ablation studies across different datasets and heterogeneous models, showing the competitive results of the proposed framework compared to state-of-the-art methods. For example, FedProtoKD achieves up to 1.13% and 34.13% accuracy improvements in the accuracy of the server model. These results demonstrate that FedProtoKD enhances class prototype separation by providing a class-wise adaptive margin, which regularizes each class based on its distribution.

II. PROBLEM FORMULATION AND MOTIVATION

A. Dual Knowledge Distillation

We utilized the dual-knowledge paradigm for distillation. By dual knowledge, we are referring to logits and prototypes here. The Logits share the local model knowledge through the unlabeled public data. The prototype is the sample-level feature representation of the user’s model on private data. Both could enhance the performance and the learning of the system.

B. Biasness of the Unlabeled Public Data on the Server

The logits of the clients in the unlabeled public data represent the local model learning based on their private data. However, the aggregated logits could express which public data samples represent more accurate information about the client’s local model. With this idea, FedPKD [18] filtered the top-performing samples based on aggregated logits and prototypes. Excluding the remaining samples increases the global model performance but makes it prone to overfitting on those samples. Furthermore, it lost the diversity of data in the system. We plan to keep all the samples in the server training to address this conflict. We place more emphasis on high-quality samples and less on low-quality samples to ensure the effectiveness of the samples according to their quality.

C. Prototype Margin Shrink and Trainable Global Prototypes

FedProto [11] used lightweight class prototypes P^c to distill client knowledge to collaboratively obtain server prototypes \tilde{P}^c . Each client c_i computes its prototype $P_{c_i}^c$ for class c using Equation (1) before sharing with the server:

$$P_{c_i}^c = \frac{1}{|D_{c_i}^c|} \sum_{(x_i, y_i) \in D_{c_i}^c} \mathcal{F}_{\theta_{c_i}}(x_i; \theta_i), \quad (1)$$

where, $D_{c_i}^c$ refers to the data samples of class c of client c_i , x is the data sample, and \mathcal{F}_{θ} is the client’s local model parameter. The client model has class prototypes with differing separability and margins in a heterogeneous model and statistical learning environment. Therefore, the vanilla weighted average FedPKD [18] of client prototypes to get aggregated server prototypes, denoted as \tilde{P}^c showed in (2), which does not adequately consider the different degrees of class separability among clients.

$$\tilde{P}^c = \frac{1}{|\mathcal{N}_c|} \sum_{i \in \mathcal{N}_c} \frac{|D_{c_i}^c|}{N_c} P_{c_i}^c, \quad (2)$$

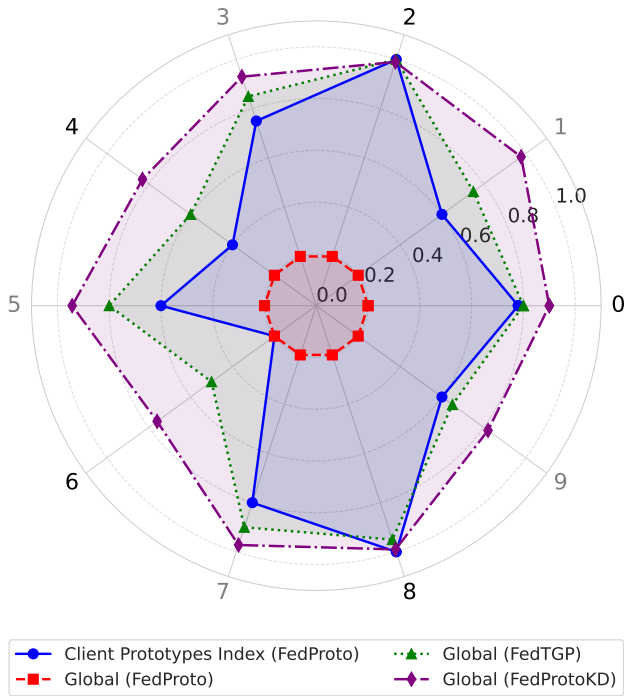


Fig. 1. The figure shows prototype margin changes after generating global prototypes. The margin is the minimum Euclidean distance between a class prototype and others, while the maximum margin is the highest among clients. To improve visualization, we normalize the margin values for each method on CIFAR-10.

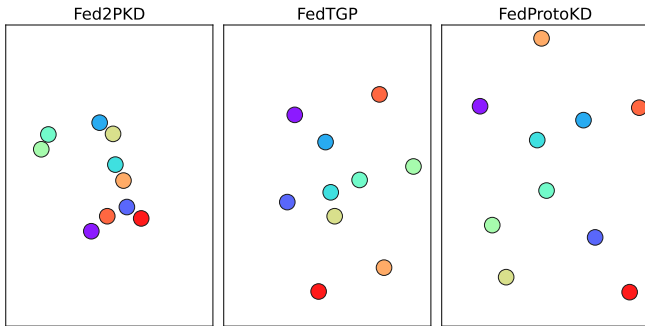


Fig. 2. Comparison of class prototypes for Fed2PKD, FedTGP, and FedProtoKD. Each point represents a class prototype. The plots illustrate the distribution and relative positioning of class prototypes, emphasizing differences in class separability

where, N_c is the number of data samples of class c in one client, \mathcal{N}_c is the number of data samples of class c across all the clients. FedPKD [18] method might give more influence (or heavier weights) to clients who perform poorly in diverse (heterogeneous) situations. FedProto [11] do vanilla averaging of the client class prototype. As a result, it can undermine the quality of the global prototypes, represented as $\tilde{\mathcal{P}}^c$, which may reduce the global prototype margin. In Figure 1, prototype margin is important because it helps keep well-performing clients distinct from others. When the margin shrinks in FedProto, it reduces the separation between classes for those good performers, causing a “prototype margin shrinking” problem that worsens

the system’s overall performance. Trainable prototypes have been introduced in FedTGP [20] during model training to tackle the margin-shrinking issue, helping to tighten up similarities within the same class (intra-class compactness) and increase the differences between classes (inter-class separation). FedTGP [20] employs an adaptive margin to enforce a better separation between prototypes of different classes via the contrastive learning phase. The server performs prototype learning solely based on the prototype data received from the clients. This approach allows the client models and global prototypes to learn independently. They used adaptive maximum margins for all class prototypes, penalizing each class similarly despite having different prototype class centers. However, they used a single max adaptive margin across all classes, which can lead to over-regularization for tightly clustered classes, pushing their prototypes unnecessarily far apart in Figure 2. The uniform margin overlooks class-specific prototype variability, reducing flexibility and impairing class alignment, particularly for classes with lower spread, which ultimately degrades model performance. We shed light on the abovementioned challenges and develop our novel idea, FedProtoKD. Our approach uses an adaptive class-wise margin $\xi^c(t)$ that dynamically adjusts throughout the training. Each class prototype is penalized by the class-specific prototype margin, which significantly impacts to generation of class-specific prototypes, which is shown in Figure 2 and the results section. Using class-wise adaptive margins allows each class prototype to be adjusted based on distribution, preventing over-regularization for tightly clustered classes, ensuring better alignment, and improving overall model performance.

D. Design of Contrastive Learning Based Generator

We generate a new set of server prototypes $\tilde{\mathcal{P}}^c$ for each class $c \in C$. First, initialize a trainable K dimensional vector $\hat{\mathcal{P}}^c \in \mathbb{R}^K$ for every class c , which serves as the foundation for the prototype. This vector $\hat{\mathcal{P}}^c$ is processed by a server-side neural network \mathcal{F} stated in [21] [22], with parameters \mathcal{F}_θ . The network \mathcal{F} transforms each $\hat{\mathcal{P}}^c$ into a more refined global prototype $\tilde{\mathcal{P}}^c$, such that $\tilde{\mathcal{P}}^c = \mathcal{F}(\hat{\mathcal{P}}^c; \mathcal{F}_\theta)$. The \mathcal{F} structure typically consists of two fully connected (FC) layers with ReLU activation between the FC layers. In particular, the parameters \mathcal{F}_θ are shared between all classes, which means that the same network is used for all classes, improving consistency during training. An adaptive class-wise margin $\xi^c(t)$ that dynamically adjusts throughout the training process is updated based on the current separability of the client prototypes. This class-wise adaptive margin will allow class-wise penalization that guides the generator to generate more robust class-label prototypes. Figure 1 illustrates that FedPKD encountered a prototype margin shrinking issue after several global rounds, hindering accurate classification. In contrast, FedProtoKD maintained a sufficiently large prototype margin to differentiate class feature representatives, enhancing learning efficiency.

III. METHODOLOGY

A. Client-Side Learning and Dual Knowledge Sharing

We assume a Federated Learning framework exists in which we have a classification task with S distinct classes. Suppose that there are C clients involved, each contributing to model training on the server. Each client $c \in C$ has a local data set D_c , with each data point x_i labeled $y_i \in S$. The local model \mathcal{F}_{θ_c} trains using private data D_c by optimizing cross-entropy loss, \mathcal{L}_{CE} :

$$\min_{\theta_c} \sum_{(x_i, y_i) \in D_c} \mathcal{L}_{CE}(\mathcal{F}_{\theta_c}(x_i), y_i). \quad (3)$$

In the next step, clients will make inferences on the unlabeled public data \mathcal{D}_p on $\mathcal{F}_{\theta_c}^t(x_i)$ and extract the logits, representing the final layer output before softmax. The prototypes present the feature space representation of the client's private dataset D_c . The client will share a prototype for each class by averaging the prototypes of all samples in the same class. For each class i , the prototype P_i^c is calculated by averaging the characteristic vectors in all samples of class i in the client's data set. A sample x_i of D_c of class i denoted as $D_c^i(x_i)$ and the embedding of the feature produced by an intermediate layer represents $P_{\theta_c}(x_i)$, which is denoted as p_i^c for all the samples of class i of the client c model $\mathcal{F}_{\theta_c}^t$. Clients will share these logits and class-label prototypes \tilde{P}^c with the server, which enables dual knowledge transfer.

B. Learnable Projection Layer to Align Prototypes

For heterogeneous models, the representative layers of the prototype features are different in shape. The DINO framework [23] uses a projection head to reduce the dimensionality of the CLS token for self-supervised learning, which is more closely aligned with this work. The DeiT model [24] also applies a projection layer to the CLS token for better efficiency in various image classification tasks. An average pooling layer was added after the feature extractor in the work [25]. Therefore, our work adds a learnable projection layer after the feature extractor to align the feature representation of heterogeneous models with an identical feature dimension K . The learnable projection layer aligns feature dimensions with a shared lower-dimensional space, essential for aggregating prototypes from different clients in federated learning. It reduces or increases dimensionality while retaining critical information, minimizing information loss during aggregation.

C. Logits Aggregation

As each client shares its logits on unlabeled public samples with the server, the server aggregates them to get the global picture. Before aggregating, we will evaluate the quality of each logit sample as it is directly related to the client's local learning. A higher variance of a logit value shows higher confidence in a sample, according to [26]. Hence, we computed the variance of each logits for each sample to measure their quality. Based on the variance, the logits will get weight while aggregating

the logits from across clients for a sample. The aggregated logits $\hat{L}^t(x_i)$ for a sample x_i are computed as:

$$\hat{L}^t(x_i) = \sum_{c \in C, x_i \in \mathcal{D}_p} \frac{\sigma^2(\mathcal{F}_{\theta_c}^t(x_i))}{\sum_{k \in C, x_i \in \mathcal{D}_p} \sigma^2(\mathcal{F}_{\theta_k}^t(x_i))} \mathcal{F}_{\theta_c}^t(x_i). \quad (4)$$

Algorithm 1 FedProtoKD

Input: Public data D_p , private data $D_c, c \in \{C\}$, server \mathcal{F}_{θ_G} , client $\mathcal{F}_{\theta_c}, c \in \{C\}$, Rounds T

Output: Server \mathcal{F}_{θ_G} , Client $\mathcal{F}_{\theta_c}, c \in \{C\}$

for $t = 0, 1, \dots, T - 1$ **do**

for each client c **in parallel do**

$t = 0, \theta_c^t \leftarrow$ Local Training on D_c^t , Eq. (3)

$t > 0, \theta_c^t \leftarrow$ Local Training on D_c^t , Eq. (19)

 Class wise avg clients prototype, $P^{c,t}$, Eq. (1)

 Send logits $\mathcal{F}_{\theta_c}^t(x_i)$ and prototype $P^{c,t}$ to server

end for

 Server aggregate clients logits, \hat{L}^t , Eq. (4)

 Server gets class-wise adaptive margin $\xi^c(t)$, Eq. (6)

 Server updates $\tilde{P}^{c,t}$ using ACTSP, Eq. (7)

 Prototype & logits-based public data filtering, Eq.(10)

$\theta_G^t \leftarrow$ Server Train $\mathcal{F}(\theta_G^t)$ on D_p , Eq. (13)

 Share server logits $\mathcal{F}_{\theta_G}^t(x_i)$ & server prototype $\tilde{P}^{c,t}$

for each client c **do in parallel do**

 Receive logits $\mathcal{F}_{\theta_G}^t(x_i)$ and server prototype $\tilde{P}^{c,t}$

$\theta_c^t \leftarrow$ update local model with $\mathcal{F}_{\theta_G}^t(x_i)$, Eq. (16)

end for

end for

return $\mathcal{F}_{\theta_G}, \mathcal{F}_{\theta_c}$

D. Adaptive Class Wise Margin-Based Trainable Server Prototype

In heterogeneous environments, simply using weighted averaging of client prototypes can be ineffective due to varying feature separability and margins across clients. Low-performing models may receive disproportionate weight, distorting well-separated global prototypes and impairing the training of more substantial clients. Inspired by the idea of [20] and face recognition techniques from [27], we developed an Adaptive Class-wise Margin-based Trainable Server Prototype (ACTSP) generation method to improve prototype separability during training. FedTGP [20] used a maximum prototype margin for all classes to generate the prototype. In ACTSP, we use adaptive class-wise prototype margin to ensure class-wise adaption, as the system is heterogeneous. Therefore, all classes should be regularized according to their class margin. However, we adjusted the formulation to the Euclidean space instead of working in an angular space. The distances of the prototypes are improved with an adaptive margin term ξ , which helps to separate the prototypes between classes while compacting the examples within classes. From [27], by modifying the distance function $\Delta(P_i^c, \tilde{P}^c)$ between the prototype P_i^c of class c of client and the server prototype \tilde{P}^c for the same class. A margin penalty ζ is introduced as a threshold to enforce that the

generated margin should not be too large. The distance-based loss is defined as [20]:

$$\mathcal{L}_{\mathcal{P}^c} = \sum_{i \in \xi^t} -\log\left(\frac{e^{-\Delta(P_i^c, \tilde{\mathcal{P}}^c) + \xi}}{e^{-\Delta(P_i^c, \tilde{\mathcal{P}}^c) + \xi} + \sum_{k' \neq k} e^{-\Delta(P_i^c, \tilde{\mathcal{P}}^{c'})}}\right). \quad (5)$$

Using Equation (5), a single maximum adaptive margin ξ across all classes can lead to over-regularization for tightly clustered classes, pushing their prototypes unnecessarily far apart. Rather than keeping the margin ξ^c fixed, we propose an adaptive class-wise margin $\xi^c(t)$ that dynamically adjusts throughout the training time, t . This adaptive margin is updated on the current separability of the client prototypes. Adaptive class-wise margins adjust the margin $\xi^c(t)$ for each class c based on the extent to which the prototypes of that class are spread out. Considering the unique distribution of each class, equation (6) keeps prototypes closer to their actual class representation, ensuring that they are not unnecessarily pushed too far apart. It prevents over-regularizing classes with less variation and gives more flexibility to those with greater spread. This approach balances maintaining the true structure of each class while ensuring enough separation from other classes, leading to better alignment and improved overall performance. A threshold parameter ζ prevents the margin from growing significantly. In each iteration, t the margin is calculated based on the distance of each center of the class:

$$\xi^c(t) = \min_{c, c' \in [C], c' \neq c} (\delta(Q_t^c, Q_t^{c'}), \zeta), \quad (6)$$

where $Q_t^c = \frac{1}{|\mathcal{P}_t^c|} \sum_{i \in \xi^t} P_t^c$. Here, the cluster center of the client prototypes for class c is $\forall c \in [C]$. We employ an adaptive margin that enforces a better separation between prototypes of different classes during the contrastive learning phase. The loss of the prototype incorporates the adaptive class-wise margin $\xi^c(t)$ and is expressed as:

$$\mathcal{L}_{\mathcal{P}^c} = \sum_{i \in \xi^t} -\log \frac{e^{-\Delta(P_i^c, \tilde{\mathcal{P}}^c) + \xi^c(t)}}{e^{-\Delta(P_i^c, \tilde{\mathcal{P}}^c) + \xi^c(t)} + \sum_{c' \neq c} e^{-\Delta(P_i^c, \tilde{\mathcal{P}}^{c'})}}. \quad (7)$$

E. Prototype and Logits-Based Public Data Quality Importance

For each public sample x_i , the server uses the aggregated global logits $\hat{L}^t(x_i)$ to identify the pseudo-label class label y_i :

$$\tilde{y}_i = \arg \max_{y_i \in [0, N-1]} \hat{L}^t(x_i). \quad (8)$$

According to this work [18], for any public sample x_i , whose feature vectors are far from the pseudo-label, global prototypes are considered low-quality samples. A class labels the feature space represented by its prototypes so that the samples of that class should be closer to its class prototypes. If a sample's feature vector's L_2 distance is close to its pseudo-label prototypes, we can consider it a high-quality sample. Those high-quality samples can enhance the performance of global models as it representative of the client's model quality. In addition, low-quality samples ensure the data diversity of the

client's private data. So, we did not discard it from the server training. We assign a certain weight to these samples while training the global model. We adjust the loss according to a factor calculated from the L_2 distance $d(x_i)$ of its feature vector and pseudo-label prototypes.

We prioritized high-quality samples and reduced the influence of less relevant samples. The authors [28] gave greater importance to the closer samples. For each samples x_i measured the inverse of L_2 distance $\hat{d}(x_i)$ for , which is given by, $\hat{d}(x_i) = \frac{1}{d(x_i) + \epsilon}$, a small constant ϵ is used to avoid division by zero. These $\hat{d}(x_i)$ inverse distances are normalized to ensure consistent scaling across the distribution. In optical loss as described by [29], samples closer in distance are given higher priority. This prioritization is controlled by a hyperparameter, φ , which determines the degree of importance assigned to each sample. Conversely, we minimized the inclusion of distant samples by applying a sigmoid scaling function, ensuring a smooth reduction centered on the median of the normalized distance C_d .

$$\mathcal{E} = 1 - \frac{1}{1 + e^{(-k \cdot (\hat{d}(x_i) - c_d))}}. \quad (9)$$

$$\mathcal{I}_i = \varphi \cdot (1 + \hat{d}(x_i)) + (1 - \varphi) \cdot \mathcal{E}, \quad (10)$$

where \mathcal{E} is the increase factor that adjusts the scale of the weights and k controls the steepness of the sigmoid curve to ensure smoothness, which refers to Curriculum Learning [30].

F. Global Model Training

The Server trains the global model with aggregated logs \hat{L}^t incorporating the importance factor \mathcal{I} of public data samples to distill the knowledge of the clients to the server. The server uses the generated trainable server prototypes $\mathcal{P}^{c,t}$ to enable the dual knowledge distillation. The Kullback–Leibler divergence (KL) loss was calculated using the aggregated logits \hat{L}_t and the server model loss and Cross-entropy (CE) loss calculated between pseudo-label y_i and the server model output $\mathcal{F}_{\theta_G}^t(x_i)$. The importance of the public sample adjusts the CE factor \mathcal{I} , allowing the server model to focus more on the most informative samples during distillation and learn about the diverse data samples, thus improving the alignment between the client and the server model. The loss of knowledge distillation \mathcal{L}_{kd} of the server model inspired from [18] is defined as:

$$\mathcal{L}_{kd} = \frac{1}{|\tilde{\mathcal{D}}_p|} \sum_{(x_i) \in \tilde{\mathcal{D}}_p} \mathcal{L}_{KL}(\hat{L}^t(x_i), \mathcal{F}_{\theta_G}^t(x_i)) + \frac{1}{|\tilde{\mathcal{D}}_p|} \sum_{(x_i, \tilde{y}_i) \in \tilde{\mathcal{D}}_p} \mathcal{L}_{CE}(\mathcal{F}_{\theta_G}^t(x_i), \tilde{y}_i) \cdot \mathcal{I}_i. \quad (11)$$

We aim to minimize the distance between the feature vectors $\mathcal{V}_{\theta_G}^t$ of each public data sample $(x_i, \tilde{y}_i) \in \tilde{\mathcal{D}}_p$ and their corresponding global pseudo-label prototypes $\mathcal{P}^{t, \tilde{y}_i}$. The focus of the mean squared error loss \mathcal{L}_{MSE} is to minimize the prototype distance and improve the alignment between the

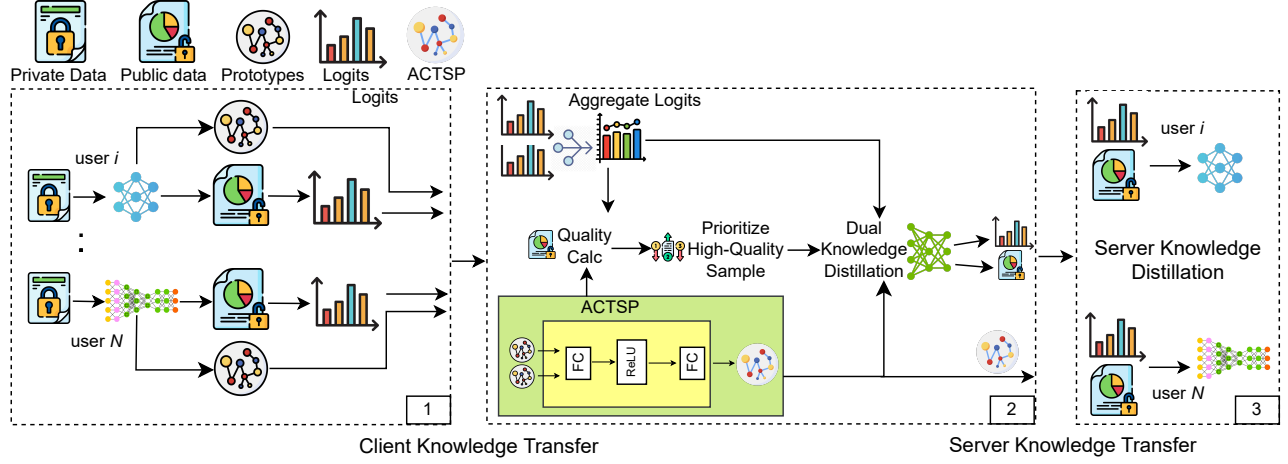


Fig. 3. Overview of the FedProtoKD framework

client and server models. The prototype loss term \mathcal{L}_{pl} in the server model training is defined as:

$$\mathcal{L}_{pl} = \frac{1}{|\tilde{\mathcal{D}}_p|} \sum_{(x_i, \tilde{y}_i) \in \tilde{\mathcal{D}}_p} \mathcal{L}_{MSE}(\mathcal{V}_{\theta_G}^t(x_i), \mathcal{P}^t, \tilde{y}_i). \quad (12)$$

The global model is optimized by solving the following objective function to minimize the loss during training inspired by [18]:

$$\mathcal{F}(\theta_G) = \mathcal{L}_{kd} \cdot \Upsilon + \mathcal{L}_{pl} \cdot (1 - \Upsilon). \quad (13)$$

G. Distill Global Knowledge Transfer to Clients

The server distills global knowledge to the clients to generalize global learning. The server only shares the logits $\mathcal{F}_{\theta_G}^t(x_i)$ of the server model and the trainable server prototypes \mathcal{P}^c . To prevent the client model from overfitting due to supervised training on limited local data and to improve the generalization of the client model, each client is trained using the public data $\tilde{\mathcal{D}}_p$ and the knowledge received from the server. The client generates a pseudo label \tilde{y}_i^s for the public samples using the server logits while training the local model. The training objective for the client inspired from [18] is defined as follows:

$$\mathcal{L}_{KL} = \sum_{(x_i, \tilde{y}_i^s) \in \tilde{\mathcal{D}}_p} \mathcal{L}_{KL}(\mathcal{F}_{\theta_c}^t(x_i), \mathcal{F}_{\theta_G}^t(x_i)). \quad (14)$$

$$\mathcal{L}_{CE} = \sum_{(x_i, \tilde{y}_i^s) \in \tilde{\mathcal{D}}_p} \mathcal{L}_{CE}(\mathcal{F}_{\theta_c}^t(x_i), \tilde{y}_i^s). \quad (15)$$

$$\min_{\theta_c} (\eta \cdot \mathcal{L}_{KL} + (1 - \eta) \cdot \mathcal{L}_{CE}). \quad (16)$$

In the initial communication round t , training is primarily based on the local data of each client using eq (3). However, starting from the subsequent rounds $t + 1$, clients are provided with global prototypes \mathcal{P}^c from the server. The training objective is then modified to include regularization, aiming to reduce the discrepancy between the client's prototypes \mathcal{P}_{θ}^c and the global prototypes \mathcal{P}^c .

$$\mathcal{L}_{CE}^{t+1} = \sum_{(x_i, y_i) \in D_c} \mathcal{L}_{CE}(\mathcal{F}_{\theta_c}^{t+1}(x_i), y_i). \quad (17)$$

$$\mathcal{L}_{MSE}^{t+1} = \sum_{(x_i, y_i) \in D_c} \mathcal{L}_{MSE}(\mathcal{P}_{\theta_c}^{t+1}(x_i), \mathcal{P}^{t, y_i}) \cdot \epsilon. \quad (18)$$

$$\min_{\theta_c} (\mathcal{L}_{CE}^{t+1} + \mathcal{L}_{MSE}^{t+1}). \quad (19)$$

IV. EXPERIMENTS DESIGN

A. Datasets

We conduct experiments on two benchmark datasets: CIFAR-10 and CIFAR-100 [31]. These are widely used benchmarks with 50,000 training and 10,000 test images, divided into 10 and 100 classes. We create a public dataset with 2,500 unlabeled samples and distribute the rest to clients for local training, simulating a non-IID federated learning environment.

B. Model and Data Heterogeneity

We employed ResNet18 and ResNet34 with 512-dimensional prototype layers alongside ResNet50, ResNet101, and ResNet152 with 2048-dimensional layers. We aligned these model dimensions using a learnable projection layer to address model heterogeneity. We use ResNet34 as the server model in all experiments. We use floating-point operations (FLOPs) counting for different models for experiments. We only consider the forward and backward passes involving the trainable parameter operations to estimate the number of FLOPs for each model. We execute all the experiments with two statistically heterogeneous settings. We use practical and pathological settings for data heterogeneity. The practical setting uses Dirichlet distribution [32] to distribute class and data samples among the clients. We use $\alpha = 0.1$ for extreme and $\alpha = 0.3$ for moderate heterogeneity. Pathological setting [1] distributes non-redundant and unbalanced data samples to clients. Each client gets $k = 3, 20$ classes for extreme heterogeneity and $k = 5, 40$ for moderate heterogeneity from the CIFAR-10 and CIFAR-100 datasets.

C. Baselines

Our study compares FedProtoKD to several state-of-the-art federated learning approaches, including various techniques designed to tackle challenges in federated learning settings.

- FedAvg [1]: An approach integrating full model updates from distributed clients in a non-heterogeneous environment to improve the global model.
- FedProto [12]: This method introduces Federated Prototype Learning, enhancing knowledge sharing in heterogeneous FL by aligning local prototypes with a globally shared prototype space and improving generalization without sharing raw model parameters.
- FedProx [34]: A federated learning framework that mitigates client heterogeneity by adding a proximal term to the local objective, stabilizing training, and improving convergence across various client devices.
- FedPKD [18]: A prototype-based ensemble distillation method filters knowledge using class-wise prototypes to select proxy samples with high-quality information for distillation.
- Fed2PKD [19]: This method uses prototypical contrastive distillation to align client embeddings with global prototypes.
- FedTGP [20]: A prototype-based federated learning system that uses a trainable global prototype using the maximum prototype margin.
- FedProtoKD- ζ : We designed another variation of FedProtoKD, using an adaptive maximum margin for all trainable server class prototypes and uses all the public samples. The performance of FedProtoKD- ζ will show the importance of class-wise adaptive margin in FedProtoKD while generating a trainable server prototype.

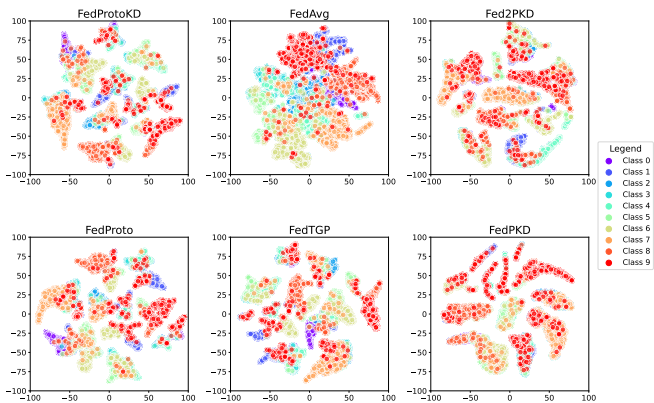


Fig. 4. visualization of the feature embeddings for different classes in CIFAR-10, $\alpha = 0.3$

D. Implementation Setup

Most experiments follow the following settings: number of clients $c = 10$, client participation ratio $\rho = 1$, clients' local model training epoch $ep_c = 5$, server model training epoch $ep_s = 10$, model training batch size $bs = 32$ in each global round, and FL communication iterations $T = 50$. The trainable

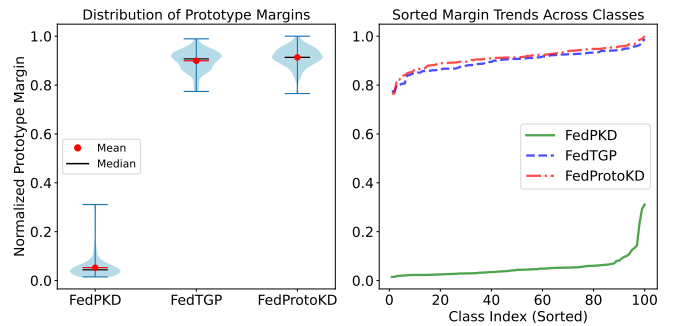


Fig. 5. Distribution and Trends of Class Prototype Margins in CIFAR-100, $\alpha = 0.1$

prototype generator uses epoch $ep_{tsp} = 100$, margin growth threshold $\zeta = 50$, and training batch size was 32. We also performed a few other experiments with different configuration values; we mentioned those setup details where needed. Each client has test data samples, and the FL server has a separate test sample set. The server test samples set has all the available classes in the system. Experiment results in Table IV and III are shown from homogeneous model settings. All other experiment results in this paper are from heterogeneous model settings.

1) *Hyperparameters*: The experiments involve several hyperparameters. We use identical feature dimensions for heterogeneous models $k = 512$, varying 256, 1024 in Table VI. We set the training parameter $\Upsilon = \epsilon = \eta = 0.5$. The default margin growing threshold generates a trainable server prototype using ACTSP $\zeta = 50$, varying from 10 to 100 in Table V. For FedPKD, we set the filter ratio for public data samples $\theta = 80\%$.

2) *Evaluation Metrics*: To evaluate the effectiveness and robustness of the system, we focus on the following metrics: (1) The enhancement of the class prototype margin in the trainable global prototype improves the classifier's ability to predict accurately by ensuring clear separation between class prototypes (2) Server model test accuracy S_{acc} on the global test data that contains all the available system classes that reflect the global generalization. (3) Client models test accuracy C_{acc} in the client's test dataset, which contains classes available in the client training dataset that provide personalized accuracy.

V. EXPERIMENTS ANALYSIS

A. Enhanced Class Prototype Margin

Figure 1 illustrates that FedProto and FedTGP face a prototype margin shrinking problem after a few global rounds, making classification more challenging. In contrast, FedProtoKD effectively enlarges the prototype margin, improving the distinction among class feature representations and learning efficiency. As shown in Figure 5, FedProtoKD utilizes ACTSP to generate a significantly more significant prototype margin than other methods, leading to improved performance. Consequently, both the server and client models outperform the baseline models. The maximum prototype margin among all classes is around 12 for FedPKD, whereas most prototype

TABLE I
SERVER TEST ACCURACY (%) UNDER EXTREME AND MODERATE HETEROGENEITY ON HETEROGENEOUS MODELS

Datasets	Extreme Data Heterogeneity				Moderate Data Heterogeneity			
	$\alpha = 0.1$		$k = 3/20$		$\alpha = 0.3$		$k = 5/40$	
	CIFAR-10	CIFAR-100	CIFAR-10	CIFAR-100	CIFAR-10	CIFAR-100	CIFAR-10	CIFAR-100
Fed2PKD	54.84	24.98	27.81	15.70	42.53	32.20	55.47	19.10
FedPKD	62.58	29.11	60.58	29.69	68.52	30.04	70.12	29.23
FedProtoKD-ζ	62.11	30.23	60.61	29.05	68.61	31.76	69.50	30.75
FedProtoKD	63.14	31.80	61.94	30.88	71.56	32.63	70.61	30.29

TABLE II
CLIENTS TEST ACCURACY (%) UNDER EXTREME AND MODERATE HETEROGENEITY ON HETEROGENEOUS MODELS

Datasets	Extreme Data Heterogeneity				Moderate Data Heterogeneity			
	$\alpha = 0.1$		$k = 3/20$		$\alpha = 0.3$		$k = 5/40$	
	CIFAR-10	CIFAR-100	CIFAR-10	CIFAR-100	CIFAR-10	CIFAR-100	CIFAR-10	CIFAR-100
FedProto	87.16	59.98	91.54	59.13	80.12	44.22	82.54	60.31
FedTGP	87.32	60.42	91.95	60.03	80.58	44.74	83.33	60.65
Fed2PKD	78.95	47.72	76.37	48.90	71.57	35.30	78.48	43.85
FedPKD	85.27	59.92	90.05	60.27	79.52	42.04	83.91	59.80
FedProtoKD-ζ	86.09	60.34	91.54	61.57	80.51	44.04	83.66	61.02
FedProtoKD	88.27	61.44	91.47	61.87	81.21	45.28	84.72	61.94

margins for FedTGP and FedProtoKD are over 30. FedProtoKD consistently outperforms both, reaching 38, followed by FedTGP, with FedPKD trailing significantly. These graphs confirm the superior performance of FedProtoKD in federated learning on CIFAR-100. FedProtoKD has a more considerable prototype margin than FedTGP and clear separation among feature embeddings in Figure 4, which shows the effectiveness of our approach. The experimental results in Tables V, present results for different margin growth thresholds $\zeta = 10, 50, 100$. Unless stated otherwise, all experiments use $\zeta = 50$ and 100 training epochs as default settings.

B. Accuracy in Heterogeneous Model Settings

We compare FedProtoKD with benchmarks supporting model heterogeneity, including FedProto, FedPKD, Fed2PKD, and FedTGP. In Tables I and II, FedProtoKD surpasses all the baselines mentioned for their extreme and moderate heterogeneous data distribution. For server model accuracy, it excels over Fed2PKD by margins of 6.82% to 34.13% across different datasets in extremely heterogeneous cases. For moderate heterogeneous cases, FedProtoKD outperforms by 2.59% to 29.03% for different datasets. This advantage continues in the client accuracy as well. Our approach outperforms all the baselines for extremely heterogeneous cases with improvements of about 9.32% to 15.1% across the mentioned datasets. While FedPKD is competitive, FedProtoKD consistently surpasses it by up to 3% in client accuracy and 2.7% in server accuracy. Also, as FedTGP performs well in heterogeneous federated learning, FedProtoKD consistently achieves higher client accuracy by up to 1.39% across various datasets and heterogeneity settings. These results highlight FedProtoKD’s superior prototype alignment, reducing class imbalance and improving FL performance on heterogeneous models.

C. Accuracy in Homogeneous Model Settings

We evaluate FedProtoKD in homogeneous model settings in clients, with Tables III and IV showing its superior accuracy for both server and client models. In extreme data heterogeneity, FedProtoKD improves server accuracy by 7.11% to 34.71%, while in moderate heterogeneity, it achieves gains of 10.38% to 35.18%. A similar trend is observed for client accuracy, with improvements ranging from 7.97% to 19.37% in moderate non-iid cases. For server accuracy FedProtoKD outperforms FedPKD in most settings, with a 0.93% gain in CIFAR-10 and a 2.29% improvement in CIFAR-100. For client accuracy, compared to FedPKD, FedProtoKD has a +1.96% gain in CIFAR-10 and a 3.06% improvement in CIFAR-100. FedProtoKD outperforms FedTGP in all cases, particularly in client accuracy for CIFAR-10 dataset, where it improves by 2.59%. The performance difference is more significant in CIFAR-100, indicating better adaptability to heterogeneous clients. The effectiveness of ACTSP is evident, as the trainable server prototype adapts better to heterogeneous data distributions, making the system more robust, even in cases where dominant model prototypes skew aggregation. In contrast, FedAvg, though effective in homogeneous federated learning, struggles in complex scenarios due to its reliance on a uniform model structure and the high computational cost of full model weight updates. FedProtoKD, being lightweight and computationally efficient, offers a superior solution for handling heterogeneous federated learning environments.

D. Robustness of the System

1) *Impact of Clients Number:* Table VI illustrates the impact of the number of clients in the system. FedProtoKD consistently outperforms across different client sizes, achieving 3.08% improvement over FedPKD when using 50 clients. Most client models utilize 512, 1024, or 2048 prototype feature dimensions, requiring dimension alignment for effective aggregation. We

TABLE III
SERVER TEST ACCURACY (%) ON MODERATE AND EXTREME DATA HETEROGENEITY ON HOMOGENEOUS MODELS

Datasets	Extreme Data Heterogeneity				Moderate Data Heterogeneity			
	$\alpha = 0.1$		$k = 3/20$		$\alpha = 0.3$		$k = 5/40$	
	CIFAR-10	CIFAR-100	CIFAR-10	CIFAR-100	CIFAR-10	CIFAR-100	CIFAR-10	CIFAR-100
FedAvg	66.21	33.98	42.40	33.67	75.48	39.12	73.97	35.63
Fed2PKD	51.55	24.63	27.45	16.54	45.53	34.45	35.75	21.73
FedPKD	61.24	30.98	61.02	30.20	71.08	31.43	69.41	31.66
FedProtoKD	62.37	31.74	62.16	31.29	70.46	33.72	70.93	32.11

TABLE IV
CLIENT TEST ACCURACY (%) UNDER EXTREME AND MODERATE DATA HETEROGENEITY ON HOMOGENEOUS MODEL

Datasets	Extreme Data Heterogeneity				Moderate Data Heterogeneity			
	$\alpha = 0.1$		$k = 3/20$		$\alpha = 0.3$		$k = 5/40$	
	CIFAR-10	CIFAR-100	CIFAR-10	CIFAR-100	CIFAR-10	CIFAR-100	CIFAR-10	CIFAR-100
FedAvg	91.19	66.53	92.97	63.17	86.38	48.96	86.38	66.17
FedProto	87.07	60.46	90.85	59.99	79.47	44.95	82.65	60.88
FedProx	86.77	60.70	90.37	59.60	80.31	44.92	81.06	60.17
Fed2PKD	81.88	47.44	76.38	52.83	73.84	37.63	64.36	51.30
FedTGP	87.83	60.14	91.42	60.93	81.14	44.10	82.58	60.82
FedPKD	86.45	59.45	91.29	59.48	81.22	43.83	82.07	59.38
FedProtoKD	88.41	62.34	92.69	62.36	82.61	45.60	83.73	62.44

incorporate a learnable projection layer in the k -dimension to achieve this, ensuring uniform prototype representation across clients. Experimental results show that FedProtoKD performs best with $k = 512$, achieving an accuracy of 71.56%, leading us to adopt this feature dimension for all experiments.

TABLE V
SERVER AND CLIENT ACCURACY (%) ON ACTSP MARGIN GROWTH THRESHOLD ζ AND EPOCH IN ACTSP FOR CIFAR-10, $\alpha = 0.1$

	Server Accuracy						
	Margin Threshold ζ			Epoch in ACTSP			
	10	50	100	50	100	500	
FedProtoKD- ζ	61.27	62.11	61.73	61.33	62.11	60.19	
FedProtoKD	62.59	63.14	63.18	62.12	63.14	63.43	
	Client Accuracy						
	FedTGP	86.36	87.32	87.90	86.18	87.32	87.27
	FedProtoKD- ζ	85.79	86.98	88.42	85.53	86.98	88.15
FedProtoKD	87.91	88.27	88.48	86.59	88.27	88.62	

TABLE VI
SERVER AND CLIENT ACCURACY (%) ON CLIENT NUMBERS AND FEATURE DIMENSIONS k IN CIFAR-10, $\alpha = 0.3$

	Server Accuracy						
	Client N			Feature Dimension k			
	10	20	50	256	512	1024	
FedPKD	68.52	68.78	61.75	70.00	68.52	66.88	
FedProtoKD- ζ	68.61	69.87	61.69	69.11	68.61	69.24	
FedProtoKD	71.56	69.97	64.83	70.34	71.56	70.21	
	Client Accuracy						
	FedProto	80.12	75.29	66.82	79.38	80.12	79.16
	FedTGP	80.58	75.80	67.84	80.76	80.58	80.13
FedPKD	79.52	73.26	63.56	79.94	79.52	79.61	
FedProtoKD- ζ	80.51	74.47	63.81	80.12	80.51	79.79	
FedProtoKD	81.21	77.18	67.98	81.38	81.21	80.98	

2) *Unlabeled Public Dataset Size*: Figure 6 presents the server’s accuracy in various public data sizes. While larger public datasets provide richer knowledge and improve performance, they also introduce higher communication overhead. We

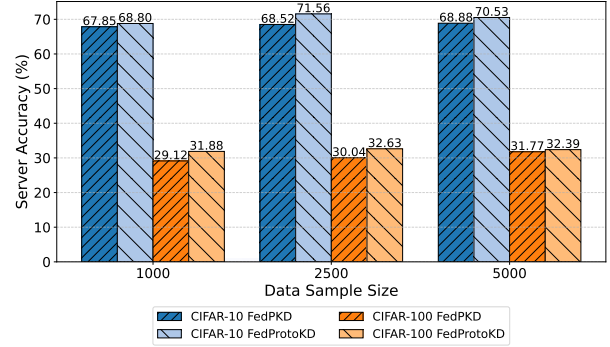


Fig. 6. Server accuracy on different public dataset sizes in CIFAR-10 and CIFAR-100, $\alpha = 0.3$

TABLE VII
CLIENT AND SERVER ACCURACY IN VARY EPOCH IN CLIENT ep_c AND SERVER ep_s TRAINING IN CIFAR-10, $\alpha = 0.3$

ep_c, ep_s	5, 10		10, 15		15, 20	
	Client	Server	Client	Server	Client	Server
FedPKD	79.52	68.52	85.36	59.10	88.19	60.21
FedProtoKD- ζ	80.51	68.61	86.21	58.28	87.46	58.36
FedProtoKD	81.21	71.56	87.96	60.92	89.43	61.53

selected a public data sample size of 2,500 to balance efficiency and accuracy as the optimal tradeoff. Table VIII demonstrates that selecting higher-importance samples enhances alignment with the class prototype. A higher $\varphi = 0.8$ (80% samples) increases accuracy, reaching 31.80% as it selects more data samples to distill the knowledge to the server.

3) *Number of Epochs in Client and Server Training*: We examine the effect of different training epochs on the local and server models in Table VII. Lower epoch numbers ensure slow learning of the local data in the server, which ensures slow convergence to the models, and that helps the global model to

learn more knowledge.

TABLE VIII
SERVER MODEL ACCURACY WITH DIFFERENT φ FRACTIONS OF SAMPLES TO PRIORITIZE IN EQUATION (10) ON FEDPROTOKD

Dataset	α	Fractions of samples, φ		
		40%	60%	80%
CIFAR-10	0.1	60.10	61.87	63.14
CIFAR-100	0.1	29.72	31.15	31.80
	k			
CIFAR-10	3	59.64	60.75	61.94
CIFAR-100	20	28.52	30.09	30.88

E. Ablation Study

We perform the ablation experiments in Table IX in two ways to see the effectiveness of the proposed approach. First, we use a maximum margin in FedProtoKD- ζ instead of the adaptive class-wise margin in ACTSP and use the importance of the public data sample \mathcal{I} . This approach demonstrates the effectiveness of assigning importance to data samples for extracting distillation knowledge. Secondly, the W/O \mathcal{I} approach states that an adaptive class-wise margin in ACTSP and uses all public samples. This approach shows the effectiveness of the adaptive class-wise margin. Lastly, we combine both approaches in FedProtoKD to see their effectiveness. For example, in CIFAR-100, We can see FedProtoKD- ζ perform 30.23% less than the W/O \mathcal{I} , which states the necessity of adaptive class-wise margin in ACTSP. In contrast, for the CIFAR-10 dataset, the adaptive class-wise margin and public sample importance similarly impact the server model performance. FedProtoKD performed better than the individual’s contribution, which proves the use of both approaches.

TABLE IX
SERVER ACCURACY FOR ABLATION STUDY IN EXTREME DATA HETEROGENEITY

Dataset	α	FedProtoKD- ζ	W/O \mathcal{I}	FedProtoKD
CIFAR-10	0.1	61.14	61.96	63.12
CIFAR-100	0.1	30.23	30.41	31.80
	k			
CIFAR-10	3	58.37	58.15	61.94
CIFAR-100	20	29.12	29.63	30.88

VI. RELATED WORK

A. Heterogeneity on FL

Statistical heterogeneity among clients, commonly referred to as the non-IID problem, presents the most significant challenge in Federated Learning. To address this challenge, FL algorithms such as FedProx [35] introduce a proximal term to the local training objective to prevent models on each client from over-fitting to their local data distribution. Some prominent approaches also addressed this problem, such as regularization [2], model mixture [36]–[38], clustering clients [39], [40], and meta-learning [41] have been introduced to stabilize the trained models. While personalized [2] and other FL methods address FL’s statistical heterogeneity, they fall short in scenarios where clients use heterogeneous models. Heterogeneous Federated

Learning (HFL) has emerged to handle both model and statistical heterogeneity, ensuring privacy protection. An HFL approach allows clients to sample diverse submodels from a shared global model, enabling flexible communication and computation [42]–[44]. Another HFL strategy involves splitting each client’s model architecture, sharing only the top layers while keeping the bottom layers distinct, as seen in methods like LG-FedAvg [45] and FedGen [46]. Despite this, sharing and aggregating top layers can result in suboptimal performance due to statistical heterogeneity [47].

B. Federated Ensemble Distillation

Knowledge Distillation can be crucial in solving Heterogeneous challenges in FL. FedDF [12] uses an ensemble of local models as a teacher to train the global model as a student, leveraging model diversity to outperform FedAvg in non-IID scenarios. FedBE [48] employs Bayesian inference to model the parameter distribution of local models. FedBE samples additional teacher models to enable robust ensemble distillation using this distribution. FedPKD [18] uses class-wise prototypes to select high-quality proxy samples for distillation, relying on public proxy data. However, it overlooks the quantitative impact of domain drift on performance.

C. Prototype Learning

The idea of prototypes, defined as the mean of multiple features, has been applied across various tasks. In image classification, a prototype represents a class, calculated as the average feature vectors within each class [49]. Several researchers [50] [11] have recently applied prototype learning to FL to enhance its performance. For instance, FedProc [51] introduced a prototypical contrastive federated learning method to improve learning in non-IID scenarios. However, FedProc does not support heterogeneous model structures across clients, as it transfers model parameters between clients and the server. FedProto [11] aggregates client prototypes for regularization but doesn’t train a model itself. ProtoFSSL [52] applies prototype learning in FSSL to generate pseudo-labels for unlabeled data. Another work, [19], introduces Fed2PKD using a two-pronged knowledge distillation approach. It integrates prototypical contrastive distillation to align client embeddings with global prototypes and semi-supervised global distillation to capture global data characteristics. FedPKD [18] uses prototype learning in FL to boost client-server model performance and reduce communication. Our work addresses these challenges by using prototypes as class representatives to tackle the prototype margin shrinking problem.

VII. CONCLUSION

This paper introduces FedProtoKD, a novel Heterogeneous Federated Learning method that addresses the prototype margin shrinking problem using class-wise adaptive margins to improve class separability. It enhances knowledge distillation by effectively managing both model and data heterogeneity while preserving client privacy. Moreover, it also finds out the importance of each public sample to amplify servers’ learning

performance. We have conducted extensive experiments and demonstrated the superiority of FedProtoKD compared to state-of-the-art benchmarks. Future work will explore larger datasets and diverse foundation models to further assess its robustness.

REFERENCES

- [1] B. McMahan, E. Moore, D. Ramage, S. Hampson, and B. A. y Arcas, "Communication-efficient learning of deep networks from decentralized data," in *Proc. Artificial Intelligence and Statistics*, 2017, pp. 1273–1282.
- [2] C. T. Dinh, N. Tran, and J. Nguyen, "Personalized federated learning with moreau envelopes," in *Advances in Neural Information Processing Systems*, vol. 33, pp. 21394–21405, 2020.
- [3] Q. Li, Y. Diao, Q. Chen, and B. He, "Federated learning on non-iid data silos: An experimental study," in *Proc. IEEE Int. Conf. Data Eng. (ICDE)*, 2022, pp. 965–978.
- [4] J. Zhang, Y. Hua, H. Wang, T. Song, Z. Xue, R. Ma, J. Cao, and H. Guan, "GPFL: Simultaneously learning global and personalized feature information for personalized federated learning," in *Proc. IEEE/CVF Int. Conf. Computer Vision*, 2023, pp. 5041–5051.
- [5] J. Zhang, Y. Hua, J. Cao, H. Wang, T. Song, Z. Xue, R. Ma, and H. Guan, "Eliminating domain bias for federated learning in representation space," in *Advances in Neural Information Processing Systems*, vol. 36, 2024.
- [6] J. Zhang, Y. Hua, H. Wang, T. Song, Z. Xue, R. Ma, and H. Guan, "Fedala: Adaptive local aggregation for personalized federated learning," in *Proc. AAAI Conf. Artificial Intelligence*, vol. 37, no. 9, pp. 11237–11244, 2023.
- [7] W. Zhuang, C. Chen, and L. Lyu, "When foundation model meets federated learning: Motivations, challenges, and future directions," *arXiv preprint arXiv:2306.15546*, 2023.
- [8] J. Zhang, Z. Gu, J. Jang, H. Wu, M. P. Stoeklin, H. Huang, and I. Molloy, "Protecting intellectual property of deep neural networks with watermarking," in *Proc. Asia Conf. Computer and Communications Security*, 2018, pp. 159–172.
- [9] L. Wang, M. Wang, D. Zhang, and H. Fu, "Model barrier: A compact untransferable isolation domain for model intellectual property protection," in *Proc. IEEE/CVF Conf. Computer Vision and Pattern Recognition*, 2023, pp. 20475–20484.
- [10] Q. Li, Z. Wen, Z. Wu, S. Hu, N. Wang, Y. Li, X. Liu, and B. He, "A survey on federated learning systems: Vision, hype and reality for data privacy and protection," *IEEE Trans. Knowl. Data Eng.*, vol. 35, no. 4, pp. 3347–3366, 2021.
- [11] Y. Tan, G. Long, L. Liu, T. Zhou, Q. Lu, J. Jiang, and C. Zhang, "Fedproto: Federated prototype learning across heterogeneous clients," in *Proc. AAAI Conf. Artificial Intelligence*, vol. 36, no. 8, pp. 8432–8440, 2022.
- [12] T. Lin, L. Kong, S. U. Stich, and M. Jaggi, "Ensemble distillation for robust model fusion in federated learning," in *Advances in Neural Information Processing Systems*, vol. 33, pp. 2351–2363, 2020.
- [13] J. Zhang, S. Guo, J. Guo, D. Zeng, J. Zhou, and A. Y. Zomaya, "Towards data-independent knowledge transfer in model-heterogeneous federated learning," *IEEE Trans. Computers*, vol. 72, no. 10, pp. 2888–2901, 2023.
- [14] L. Zhang, L. Shen, L. Ding, D. Tao, and L. Y. Duan, "Fine-tuning global model via data-free knowledge distillation for non-iid federated learning," in *Proc. IEEE/CVF Conf. Computer Vision and Pattern Recognition*, 2022, pp. 10174–10183.
- [15] C. Wu, F. Wu, L. Lyu, Y. Huang, and X. Xie, "Communication-efficient federated learning via knowledge distillation," *Nature Communications*, vol. 13, no. 1, pp. 2032, 2022.
- [16] Y. Tan, G. Long, J. Ma, L. Liu, T. Zhou, and J. Jiang, "Federated learning from pre-trained models: A contrastive learning approach," in *Advances in Neural Information Processing Systems*, vol. 35, pp. 19332–19344, 2022.
- [17] K. Zhang and Y. Sato, "Semantic image segmentation by dynamic discriminative prototypes," *IEEE Trans. Multimedia*, vol. 26, pp. 737–749, 2023.
- [18] F. Lyu, C. Tang, Y. Deng, T. Liu, Y. Zhang, and Y. Zhang, "A prototype-based knowledge distillation framework for heterogeneous federated learning," in *Proc. IEEE Int. Conf. Distributed Computing Systems (ICDCS)*, 2023, pp. 1–11.
- [19] Z. Xie, H. Xu, X. Gao, J. Jiang, and R. Han, "Fed2PKD: Bridging model diversity in federated learning via two-pronged knowledge distillation," in **2024 IEEE 17th International Conference on Cloud Computing (CLOUD)**, pp. 1–11, 2024, IEEE.
- [20] J. Zhang, Y. Liu, Y. Hua, and J. Cao, "FEDTGP: Trainable Global Prototypes with Adaptive-Margin-Enhanced Contrastive Learning for Data and Model Heterogeneity in Federated Learning," in *Proc. AAAI Conf. Artif. Intell.*, 2024, vol. 38, no. 15, pp. 16768–16776.
- [21] H. Y. Chen and W. L. Chao, "On bridging generic and personalized federated learning for image classification," *arXiv preprint arXiv:2107.00778*, 2021.
- [22] A. Shamsian, A. Navon, E. Fetaya, and G. Chechik, "Personalized federated learning using hypernetworks," in *Proc. Int. Conf. Mach. Learn. (ICML)*, PMLR, Jul. 2021, pp. 9489–9502.
- [23] M. Caron, H. Touvron, I. Misra, H. Jégou, J. Mairal, P. Bojanowski, and A. Joulin, "Emerging properties in self-supervised vision transformers," in **Proceedings of the IEEE/CVF International Conference on Computer Vision**, pp. 9650–9660, 2021.
- [24] H. Touvron, M. Cord, M. Douze, F. Massa, A. Sablayrolles, and H. Jégou, "Training data-efficient image transformers & distillation through attention," in **International Conference on Machine Learning**, pp. 10347–10357, 2021, PMLR.
- [25] C. Szegedy, W. Liu, Y. Jia, P. Sermanet, S. Reed, D. Anguelov, D. Erhan, V. Vanhoucke, and A. Rabinovich, "Going deeper with convolutions," in **Proceedings of the IEEE Conference on Computer Vision and Pattern Recognition**, pp. 1–9, 2015.
- [26] C. Gómez, S. S. Sanz, and D. Camacho, "A Review on Ensemble Methods and Their Applications to Optimization Problems," in *Springer Tracts in Nature-Inspired Computing*, 2021, pp. 25–45.
- [27] J. Deng, J. Guo, N. Xue, and S. Zafeiriou, "ArcFace: Additive Angular Margin Loss for Deep Face Recognition," in *Proc. IEEE/CVF Conf. Comput. Vis. Pattern Recognit. (CVPR)*, 2019, pp. 4690–4699.
- [28] F. Schroff, D. Kalenichenko, and J. Philbin, "FaceNet: A Unified Embedding for Face Recognition and Clustering," in *Proc. IEEE Conf. Comput. Vis. Pattern Recognit. (CVPR)*, 2015, pp. 815–823.
- [29] T. Y. Lin, P. Goyal, R. Girshick, K. He, and P. Dollár, "Focal Loss for Dense Object Detection," in *Proc. IEEE Int. Conf. Comput. Vis. (ICCV)*, 2017, pp. 2980–2988.
- [30] Y. Bengio, J. Louradour, R. Collobert, and J. Weston, "Curriculum Learning," in *Proc. 26th Int. Conf. Mach. Learn. (ICML)*, 2009, pp. 41–48.
- [31] A. Krizhevsky and G. Hinton, "Learning multiple layers of features from tiny images," in *Technical Report*, University of Toronto, 2009.
- [32] Q. Li, B. He, and D. Song, "Model-contrastive federated learning," in *Proc. IEEE/CVF Conf. Comput. Vis. Pattern Recognit.*, 2021, pp. 10713–10722.
- [33] A. Bakhtiarnia, Q. Zhang, and A. Iosifidis, "Single-layer vision transformers for more accurate early exits with less overhead," *Neural Networks*, vol. 153, pp. 461–473, 2022.
- [34] T. Li, A. K. Sahu, M. Zaheer, M. Sanjabi, A. Talwalkar, and V. Smith, "Federated optimization in heterogeneous networks," in *Proc. Machine Learning and Systems*, vol. 2, pp. 429–450, 2020.
- [35] T. Li, A. K. Sahu, M. Zaheer, M. Sanjabi, A. Talwalkar, and V. Smith, "Federated optimization in heterogeneous networks," *Proc. Mach. Learning Systems*, vol. 2, pp. 429–450, 2020.
- [36] Y. Deng, M. M. Kamani, and M. Mahdavi, "Adaptive personalized federated learning," *arXiv preprint arXiv:2003.13461*, 2020.
- [37] Y. Mansour, M. Mohri, J. Ro, and A. T. Suresh, "Three approaches for personalization with applications to federated learning," *arXiv preprint arXiv:2002.10619*, 2020.
- [38] F. Hanzely and P. Richtarik, "Federated learning of a mixture of global and local models," *arXiv preprint arXiv:2002.05516*, 2020.
- [39] F. Sattler, K.-R. Müller, and W. Samek, "Clustered federated learning: Model-agnostic distributed multitask optimization under privacy constraints," *IEEE Trans. Neural Netw. Learn. Syst.*, vol. 32, no. 8, pp. 3710–3722, 2020.
- [40] Y. J. Cho, J. Wang, T. Chiruvolu, and G. Joshi, "Personalized federated learning for heterogeneous clients with clustered knowledge transfer," *arXiv preprint arXiv:2109.08119*, 2021.
- [41] A. Fallah, A. Mokhtari, and A. Ozdaglar, "Personalized federated learning with theoretical guarantees: A model-agnostic meta-learning approach," *Advances in Neural Information Processing Systems*, vol. 33, pp. 3557–3568, 2020.

- [42] E. Diao, J. Ding, and V. Tarokh, "HeteroFL: Computation and communication efficient federated learning for heterogeneous clients," *arXiv preprint arXiv:2010.01264*, 2020.
- [43] S. Horvath, S. Laskaridis, M. Almeida, I. Leontiadis, S. Venieris, and N. Lane, "Fjord: Fair and accurate federated learning under heterogeneous targets with ordered dropout," *Advances in Neural Information Processing Systems*, vol. 34, pp. 12876–12889, 2021.
- [44] D. Wen, K.-J. Jeon, and K. Huang, "Federated dropout—A simple approach for enabling federated learning on resource constrained devices," *IEEE Wireless Commun. Lett.*, vol. 11, no. 5, pp. 923–927, 2022.
- [45] P. P. Liang, T. Liu, Z. Liu, N. B. Allen, R. P. Auerbach, D. Brent, R. Salakhutdinov, and L.-P. Morency, "Think locally, act globally: Federated learning with local and global representations," *arXiv preprint arXiv:2001.01523*, 2020.
- [46] Z. Zhu, J. Hong, and J. Zhou, "Data-free knowledge distillation for heterogeneous federated learning," in *Proc. Int. Conf. Machine Learning*, 2021, pp. 12878–12889.
- [47] Z. Li, X. Shang, R. He, T. Lin, and C. Wu, "No fear of classifier biases: Neural collapse inspired federated learning with synthetic and fixed classifier," in *Proc. IEEE/CVF Int. Conf. Computer Vision*, 2023, pp. 5319–5329.
- [48] H.-Y. Chen and W.-L. Chao, "FedBE: Making bayesian model ensemble applicable to federated learning," *arXiv preprint arXiv:2009.01974*, 2020.
- [49] J. Snell, K. Swersky, and R. Zemel, "Prototypical networks for few-shot learning," in *Advances in Neural Information Processing Systems*, vol. 30, 2017.
- [50] Q. Li, B. He, and D. Song, "Model-contrastive federated learning," in *Proc. IEEE/CVF Conf. Computer Vision and Pattern Recognition*, 2021, pp. 10713–10722.
- [51] X. Mu, Y. Shen, K. Cheng, X. Geng, J. Fu, T. Zhang, and Z. Zhang, "FedProc: Prototypical contrastive federated learning on non-iid data," *Future Gener. Comput. Syst.*, vol. 143, pp. 93–104, 2023.
- [52] W. Kim, K. Park, K. Sohn, R. Shu, and H.-S. Kim, "Federated semi-supervised learning with prototypical networks," *arXiv preprint arXiv:2205.13921*, 2022.